arXiv:0811.2880v1 [nucl-th] 18 Nov 2008

Isospin Dynamics in Heavy Ion Collisions: from Coulomb Barrier to Quark Gluon Plasma

M. Di Toro,[1,2] V. Baran,[3] M. Colonna,[2] G. Ferini ,[2]
T. Gaitanos,[4] V. Giordano,[1,2] V. Greco,[1,2] Liu Bo,[5] M. Zielinska-Pfabe,[6]
S. Plumari,[1,7] V. Prassa,[8] C. Rizzo,[1,2] J. Rizzo,[1,2] and H. H. Wolter,[9]

[1]Dipartimento di Fisica e Astronomia dell'Università, Catania, Italy
[2]INFN, Laboratori Nazionali del Sud, Catania, Italy
[3]Dept. of Theoretical Physics, Bucharest Univ. and NIPNE-HH, Romania
[4] Institute for Theoretical Physics, Giessen University, Germany
[5] IHEP, Chinese Academy of Science, Beijing, China
[6] Smith College, Northampton, Mass., USA
[7] INFN, Sezione di Catania, Italy
[8] Physics Department, Aristotles Univ.of Thessaloniki, Grece
[9] Department für Physik, Unversität Munchen, Garching, Germany

November 18, 2008

Abstract

Heavy Ion Collisions (HIC) represent a unique tool to probe the in-medium nuclear interaction in regions away from saturation. In this report we present a selection of new reaction observables in dissipative collisions particularly sensitive to the symmetry term of the nuclear Equation of State ($Iso-EoS$). We will first discuss the Isospin Equilibration Dynamics. At low energies this manifests via the recently observed Dynamical Dipole Radiation, due to a collective neutron-proton oscillation with the symmetry term acting as a restoring force. At higher beam energies Iso-EoS effects will be seen in Imbalance Ratio Measurements, in particular from the correlations with the total kinetic energy loss. For fragmentation reactions in central events we suggest to look at the coupling between isospin distillation and radial flow. In Neck Fragmentation reactions important $Iso-EoS$ information can be obtained from the correlation between isospin content and alignement. The high density symmetry term can be probed from isospin effects on heavy ion reactions at relativistic energies (few $AGeV$ range). Rather isospin sensitive observables are proposed from nucleon/cluster emissions, collective flows and meson production. The possibility to shed light on the controversial neutron/proton effective mass splitting in asymmetric matter is also suggested. A large symmetry repulsion at high baryon density will also lead to an "earlier" hadron-deconfinement transition in n-rich matter. A suitable treatment of the isovector interaction in the partonic EoS appears very relevant.

1 Introduction: The Elusive Symmetry Term of the EoS

The symmetry energy E_{sym} appears in the energy density $\epsilon(\rho,\rho_3) \equiv \epsilon(\rho) + \rho E_{sym}(\rho_3/\rho)^2 + O(\rho_3/\rho)^4 + ..$, expressed in terms of total ($\rho = \rho_p + \rho_n$) and isospin ($\rho_3 = \rho_p - \rho_n$) densities. The symmetry term gets a kinetic contribution directly from basic Pauli correlations and a potential part from the highly controversial isospin dependence of the effective interactions. Both at sub-saturation and supra-saturation densities, predictions based of the existing many-body techniques diverge rather widely, see [1, 2].

We recall that the knowledge of the EoS of asymmetric matter is very important at low densities (e.g. neutron skins, pigmy resonances, nuclear structure at the drip lines, neutron distillation in fragmentation, neutron star formation and crust) as well as at high densities (e.g. neutron star mass-radius relation, cooling, hybrid structure, transition to a deconfined phase, formation of black holes). Several observables which are sensitive to the Iso-EoS and testable experimentally, have been suggested [3, 4, 5, 6, 7, 8]. We take advantage of new opportunities in theory (development of rather reliable microscopic transport codes for HIC) and in experiments (availability of very asymmetric radioactive beams, improved possibility of measuring event-by-event correlations) to present new results that are constraining the existing effective interaction models. We will discuss dissipative collisions in a wide range of beam energies, from just above the Coulomb barrier up to the $AGeV$ range. Isospin effects on the chiral/deconfinement transition at high baryon density will be also discussed. Low to Fermi energies will bring information on the symmetry term around (below) normal density, while intermediate energies will probe high density regions. The transport codes are based on mean field theories, with correlations included via hard nucleon-nucleon elastic and inelastic collisions and via stochastic forces, selfconsistently evaluated from the mean phase-space trajectory, see [5, 9, 10, 11]. Stochasticity is essential in order to get distributions as well as to allow the growth of dynamical instabilities.

Relativistic collisions are described via a fully covariant transport approach, related to an effective field exchange model, where the relevant degrees of freedom of the nuclear dynamics are accounted for [5, 12, 13, 14, 15, 16]. We will have a propagation of particles suitably dressed by self-energies that will influence collective flows and in medium nucleon-nucleon inelastic cross sections. The construction of an $Hadron - EoS$ at high baryon and isospin densities will finally allow the possibility of developing a model of a hadron-deconfinement transition at high density for an asymmetric matter [17]. The problem of a correct treatment of the isospin in a effective partonic $E0S$ will be stressed.

We will always test the sensitivity of our simulation results to different choices of the density and momentum dependence of the Isovector part of the Equation of State ($Iso-EoS$). In the non-relativistic frame the potential part of the symmetry energy, $C(\rho)$, [5]:

$$\frac{E_{sym}}{A} = \frac{E_{sym}}{A}(kin) + \frac{E_{sym}}{A}(pot) \equiv \frac{\epsilon_F}{3} + \frac{C(\rho)}{2\rho_0}\rho \tag{1}$$

is tested by employing two different density parametrizations, Isovector Equation of State (Iso-Eos) [3, 18], of the mean field: i) $\frac{C(\rho)}{\rho_0} = 482 - 1638\rho$, ($MeVfm^3$), for "Asysoft" EoS: $E_{sym}/A(pot)$ has a weak density dependence close to the saturation, with an almost flat behavior below ρ_0 and even decreasing at suprasaturation; ii) a constant coefficient, $C = 32MeV$, for the "Asystiff" EoS choice: the interaction part of the symmetry term displays a linear dependence with the density, i.e. with a faster decrease at lower densities and much stiffer above saturation. The isoscalar section of the EoS is the same in both cases, fixed requiring that the saturation properties of symmetric nuclear matter with a compressibility around $220MeV$ are reproduced.

2 Isospin Equilibration

2.1 The Prompt Dipole γ-Ray Emission

The possibility of an entrance channel bremsstrahlung dipole radiation due to an initial different N/Z distribution was suggested at the beginning of the nineties [19, 20]. After several experimental evidences, in fusion as well as in deep-inelastic reactions, [21, 22] and refs. therein, we have now a good understanding of the process and stimulating new perspectives from the use of radioactive beams.

During the charge equilibration process taking place in the first stages of dissipative reactions between colliding ions with different N/Z ratios, a large amplitude dipole collective motion develops in the composite dinuclear system, the so-called Dynamical Dipole mode. This collective dipole gives rise to a prompt γ-ray emission which depends: i) on the absolute value of the intial dipole moment

$$D(t=0) = \frac{NZ}{A}\,|R_Z(t=0) - R_N(t=0)| = \frac{R_P + R_T}{A} Z_P Z_T \left|(\frac{N}{Z})_T - (\frac{N}{Z})_P\right|, \quad (2)$$

being $R_Z = \frac{\Sigma_i x_i(p)}{Z}$ and $R_N = \frac{\Sigma_i x_i(n)}{N}$ the center of mass of protons and of neutrons respectively, while R_P and R_T are the projectile and target radii; ii) on the fusion/deep-inelastic dynamics; iii) on the symmetry term, below saturation, that is acting as a restoring force.

A detailed description is obtained in mean field transport approaches, [23, 24]. We can follow the time evolution of the dipole moment in the r-space, $D(t) = \frac{NZ}{A}(R_Z - R_N)$ and in $p-$space, $DK(t) = (\frac{P_p}{Z} - \frac{P_n}{N})$, with P_p (P_n) center of mass in momentum space for protons (neutrons), just the canonically conjugate momentum of the $D(t)$ coordinate, i.e. as operators $[D(t), DK(t)] = i\hbar$. A nice "spiral-correlation" clearly denotes the collective nature of the mode, see Fig.1.

We can directly apply a bremsstrahlung approach, to the dipole evolution given from the Landau-Vlasov transport [24], to estimate the "prompt" photon emission probability ($E_\gamma = \hbar\omega$):

$$\frac{dP}{dE_\gamma} = \frac{2e^2}{3\pi\hbar c^3 E_\gamma} |D''(\omega)|^2, \quad (3)$$

where $D''(\omega)$ is the Fourier transform of the dipole acceleration $D''(t)$. We remark that in this way it is possible to evaluate, in *absolute* values, the corresponding pre-equilibrium photon emission.

We must add a couple of comments of interest for the experimental selection of the Dynamical Dipole: i) The centroid is always shifted to lower energies (large deformation of the dinucleus); ii) A clear angular anisotropy should be present since the prompt mode has a definite axis of oscillation (on the reaction plane) at variance with the statistical GDR. In a recent experiment the prompt dipole radiation has been investigated with a 4π gamma detector. A strong dipole-like photon angular distribution $(\theta_\gamma) = W_0[1 + a_2 P_2(cos\theta_\gamma)]$, θ_γ being the angle between the emitted photon and the beam axis, has been observed, with the a_2 parameter close to -1, see [22].

At higher beam energies we expect a decrease of the direct dipole radiation for two main reasons both due to the increasing importance of hard NN collisions: i) a larger fast nucleon emission that will equilibrate the isospin during the dipole oscillation; ii) a larger damping of the collective mode due to np collisions.

The use of unstable neutron rich projectiles would largely increase the effect, due to the possibility of larger entrance channel asymmetries [25]. In order to suggest proposals for the new RIB facility *Spiral* 2, [26] we have studied fusion events in the reaction $^{132}Sn + ^{58}Ni$ at $10AMeV$, [25, 27]. We espect a $Monster$ Dynamical Dipole, the initial dipole moment $D(t=0)$ being of the order of 50fm, about two times the largest values probed so far, allowing a detailed study of the symmetry potential,

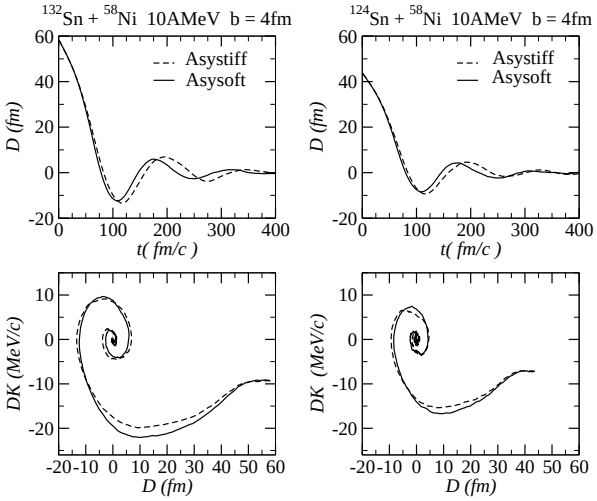

Figure 1: Dipole Dynamics at 10AMeV, $b = 4fm$ centrality. Left Panels: Exotic "132" system. Upper: Time evolution of dipole moment D(t) in real space; Lower: Dipole phase-space correlation (see text). Right Panels: same as before for the stable "124" system. Solid lines correspond to Asysoft EoS, the dashed to Asystiff EoS.

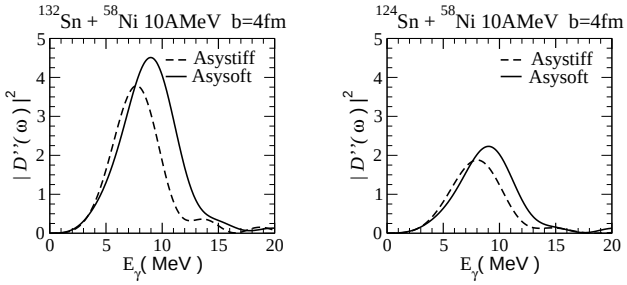

Figure 2: Left Panel, Exotic "132" system. Power spectra of the dipole acceleration at $b = 4$fm (in c^2 units). Right Panel: Corresponding results for the stable "124" system. Solid lines correspond to Asysoft EoS, the dashed to Asystiff EoS.

below saturation, responsible of the restoring force of the dipole oscillation and even of the damping, via the fast neutron emission.

In Figure 1 we report some global informations concerning the dipole mode in entrance channel. In the Left-Upper panel we have the time evolution of the dipole moment $D(t)$ for the "132" system at $b = 4fm$. We notice the large amplitude of the first oscillation but also the delayed dynamics for the Asystiff EOS related to a weaker isovector restoring force. The phase space correlation (spiraling) between $D(t)$ and $DK(t)$, is reported in Fig.1 (Left-Lower). It nicely points out a collective behavior which initiates very early, with a dipole moment still close to the touching configuration value reported above. This can be explained by the fast formation of a well developed neck mean field which sustains the collective dipole oscillation in the dinuclear configuration.

The role of a large charge asymmetry between the two colliding nuclei can be seen from Fig.1 (Right Panels), where we show the analogous dipole phase space trajectories for the stable $^{124}Sn+^{58}Ni$ system at the same value of impact parameter and energy. A clear reduction of the collective behavior is evidenced.

In Fig. 2(Left Panel) we report the power spectrum, $\mid D''(\omega) \mid^2$ in semicentral "132" reactions, for different $Iso - EoS$ choices. The gamma multiplicity is simply related to it, see Eq.(3). The corresponding results for the stable "124" system are drawn in the Right Panel. As expected from the larger initial charge asymmetry, we clearly see an increase of the Prompt Dipole Emission for the

exotic n-rich beam. Such entrance channel effect will be enhanced, allowing a better observation of the Iso-EoS dependence. In fact from Fig.2 we see also other isospin effects.

A detailed analysis can be performed just using a simple damped oscillator model for the dipole moment $D(t) = D(t_0)e^{i(\omega_0+i/\tau)t}$, where $D(t_0)$ is the value at the onset of the collective dinuclear response, ω_0 the frequency and τ the damping rate.The power spectrum of the dipole acceleration is given by

$$\mid D''(\omega) \mid^2 = \frac{(\omega_0^2 + 1/\tau^2)^2 D(t_0)^2}{(\omega - \omega_0)^2 + 1/\tau^2} \tag{4}$$

which from Eq.(3) leads to a total yield proportional to $\omega_0\tau(\omega_0^2 + 1/\tau^2)D(t_0)^2 \simeq \omega_0^3\tau D(t_0)^2$ since $\omega_0\tau > 1$. We remind that in the Asystiff case we have a weaker restoring force for the dynamical dipole in the dilute "neck" region, where the symmetry energy is smaller [5]. This is reflected in lower values of the centroids as well as in reduced total yields, as shown in Fig.2. The sensitivity of ω_0 to the stiffness of the symmetry energy will be amplified by the increase of $D(t_0)$ when we use exotic, more asymmetric beams.

The prompt dipole radiation angular distribution is the result of the interplay between the collective oscillation life-time and the dinuclear rotation. In this sense we expect also a sensitivity to the $Iso-Eos$ of the anusotropy, in particular for high spin event selections, [28].

In the Asysoft choice we expect also larger widths of the "resonance" due to the larger fast neutron emission. We note the opposite effect of the Asy-stiffness on neutron vs proton emissions. The latter point is important even for the possibility of an independent test just measuring the N/Z of the pre-equilibrium nucleon emission, [29].

2.2 Isospin Equilibration at the Fermi Energies

In this energy range the doorway state mechanism of the Dynamical Dipole will disappear and so we can study a direct isospin transport in binary events. This can be discussed in a compact way by means of the chemical potentials for protons and neutrons as a function of density ρ and isospin I [30]. The p/n currents can be expressed as

$$\mathbf{j}_{p/n} = D^{\rho}_{p/n}\nabla\rho - D^{I}_{p/n}\nabla I \tag{5}$$

with $D^{\rho}_{p/n}$ the drift, and $D^{I}_{p/n}$ the diffusion coefficients for transport, which are given explicitely in ref. [30]. Of interest here are the differences of currents between protons and neutrons which have a simple relation to the density dependence of the symmetry energy

$$\begin{aligned} D^{\rho}_n - D^{\rho}_p &\propto 4I\frac{\partial E_{sym}}{\partial\rho}\,, \\ D^{I}_n - D^{I}_p &\propto 4\rho E_{sym}\,. \end{aligned} \tag{6}$$

Thus the isospin transport due to density gradients, i.e. isospin migration, depends on the slope of the symmetry energy, or the symmetry pressure, while the transport due to isospin concentration gradients, i.e. isospin diffusion, depends on the absolute value of the symmetry energy.

We can discuss the asymmetries of the various parts of the reaction system (gas, PLF/TLF's , and in the case of ternary events, IMF's). In particular, we study the so-called Imbalance Ratio [31], which is defined as

$$R^{x}_{P,T} = \frac{2(x^M - x^{eq})}{(x^H - x^L)}\,, \tag{7}$$

with $x^{eq} = \frac{1}{2}(x^H + x^L)$. Here, x is an isospin sensitive quantity that has to be investigated with respect to equilibration. In this work we consider primarily the asymmetry $\beta = (N-Z)/(N+Z)$, but also other quantities, such as isoscaling coefficients, ratios of production of light fragments, etc, can be of

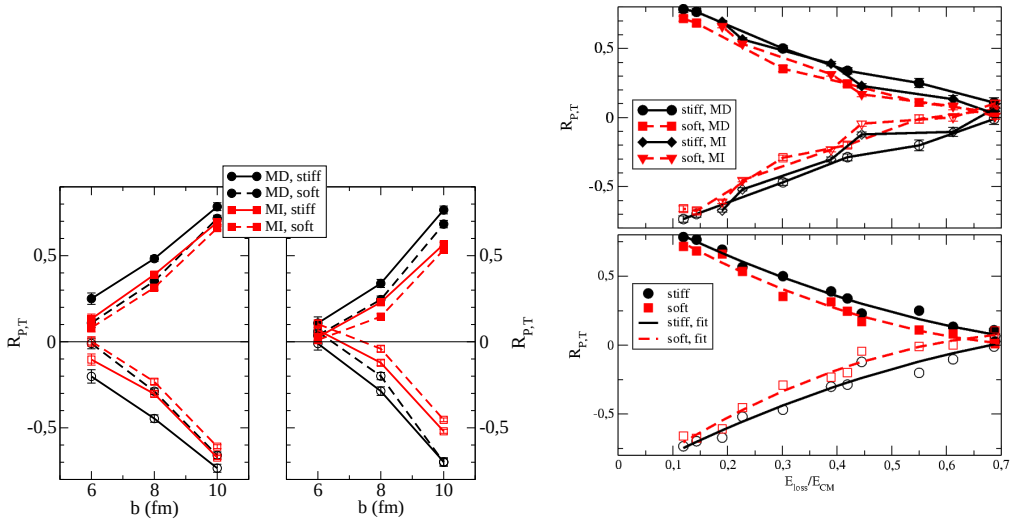

Figure 3: Left Panel.Imbalance ratios for $Sn + Sn$ collisions for incident energies of 50 (left) and 35 $AMeV$ (right) as a function of the impact parameter. Signatures of the curves: iso-EoS stiff (solid lines), soft (dashed lines); MD interaction (circles), MI interaction (squares); projectile rapidity (full symbols, upper curves), target rapidity (open symbols, lower curves). Right Panel. Imbalance ratios as a function of relative energy loss for both beam energies. Upper: Separately for stiff (solid) and soft (dashed) iso-EoS, and for MD (circles and squares) and MI (diamonds and triangles) interactions, in the projectile region (full symbols) and the target region (open symbols). Lower: Quadratic fit to all points for the stiff (solid), resp. soft (dashed) iso-EoS.

interest [7]. The indices H and L refer to the symmetric reaction between the heavy (n-rich) and the light (n-poor) systems, while M refers to the mixed reaction. P, T denote the rapidity region, in which this quantity is measured, in particular the PLF and TLF rapidity regions. Clearly, this ratio is ± 1 in the projectile and target regions, respectively, for complete transparency, and oppositely for complete rebound, while it is zero for complete equilibration.

In a simple model we can show that the imbalance ratio mainly depends on two quantities: the strength of the symmetry energy and the interaction time between the two reaction partners. Let us take, for instance, the asymmetry β of the PLF (or TLF) as the quantity x. As a first order approximation, in the mixed reaction this quantity relaxes towards its complete equilibration value, $\beta_{eq} = (\beta_H + \beta_L)/2$ as

$$\beta^M_{P,T} = \beta^{eq} + (\beta^{H,L} - \beta^{eq})\ e^{-t/\tau}, \tag{8}$$

where t is the time elapsed while the reaction partners are interacting (interaction time) and the damping τ is mainly connected to the strength of the symmetry energy. Inserting this expression into Eq.(7), one obtains $R^{\beta}_{P,T} = \pm e^{-t/\tau}$ for the PLF and TLF regions, respectively. Hence the imbalance ratio can be considered as a good observable to trace back the strength of the symmetry energy from the reaction dynamics provided a suitable selection of the interaction time is performed.

The centrality dependence of the Imbalance Ratio, for (Sn,Sn) collisions, has been investigated in experiments [32] as well as in theory [30, 33]. We propose here a new analysis which appears experimentally more selective. The interaction time certainly influences the amount of isospin equilibration, see Eq.(6) and refs. [30, 34]. Longer interaction times should be correlated to a larger dissipation. It is then natural to look at the correlation between the imbalance ratio and the total kinetic energy loss. In this way we can also better disentangle dynamical effects of the isoscalar and isovector part of the EoS, see [34].

It is seen in Fig.3 that the curves for the *asy-soft* EoS (dashed) are generally lower in the projectile

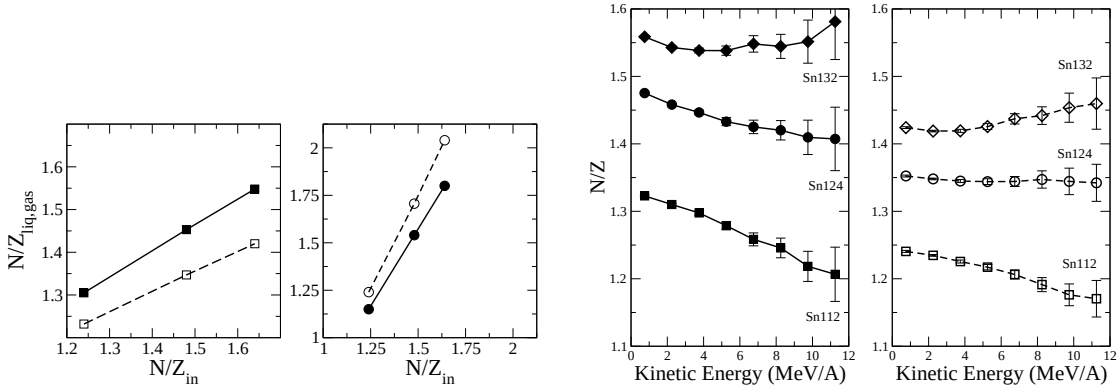

Figure 4: Left Panel.The N/Z of the liquid (left) and of the gas (right) phase is displayed as a function of the system initial N/Z. Full lines and symbols refer to the asystiff parameterization. Dashed lines and open symbols are for asysoft. Right Panel. The fragment N/Z (see text) as a function of the kinetic energy. Left: Asystiff; Right: Asysoft.

region (and oppositely for the target region), i.e. show more equilibration, than those for the *asy-stiff* EoS. In order to emphasize this trend we have, in the lower panel of the figure, collected together all the values for the stiff (circles) and the soft (squares) iso-EoS, and fitted them by a quadratic curve. It is seen that this fit gives a good representation of the trend of the results.

The difference between the curves for the stiff and soft iso-EOS in the lower panel then isolates the influence of the iso-EoS from kinematical effects associated with the interaction time. It is seen, that there is a systematic effect of the symmetry energy of the order of about 20 percent, which should be measurable. The correlation suggested in Fig.3 should represent a general feature of isospin diffusion, and it would be of great interest to verify experimentally.

3 Isospin Distillation with Radial Flow

In central collisions at 30-50 MeV/A, where the full disassembly of the system into many fragments is observed, one can study specifically properties of liquid-gas phase transitions occurring in asymmetric matter [35, 36, 37, 11, 5]. For instance, in neutron-rich matter, phase co-existence leads to a different asymmetry in the liquid and gaseous phase: fragments (liquid) appear more symmetric with respect to the initial matter, while light particles (gas) are more neutron-rich. The amplitude of this effect depends on specific properties of the isovector part of the nuclear interaction, namely on the value and the derivative of the symmetry energy at low density.

This investigation is interesting in a more general context: In heavy ion collisions the dilute phase appears during the expansion of the interacting matter. Thus we study effects of the coupling of expansion, fragmentation and distillation in a two-component (neutron-proton) system [38] .

We focus on central collisions, $b = 2\ fm$, considering symmetric reactions between systems having three different initial asymmetry: $^{112}Sn +^{112} Sn, ^{124}Sn +^{124} Sn, ^{132}Sn +^{132} Sn$, with $(N/Z)_{in} =$ 1.24,1.48,1.64, respectively. The considered beam energy is 50 MeV/A. 1200 events have been run for each reaction and for each of the two symmetry energies adopted (asy-soft and asystiff, see before) [38]. The average N/Z of emitted nucleons (gas phase) and Intermediate Mass Fragments (IMF) is presented in Fig.4 (Left Panel) as a function of the initial $(N/Z)_{in}$ of the three colliding systems. One observes a clear Isospin-Distillation effect, i.e. the gas phase (right) more neutron-rich than the IMF's (left). This is particular evident in the Asysoft case due to the larger value of the symmetry energy at low density [5].

In central collisions, after the initial collisional shock, the system expands and breaks up into many

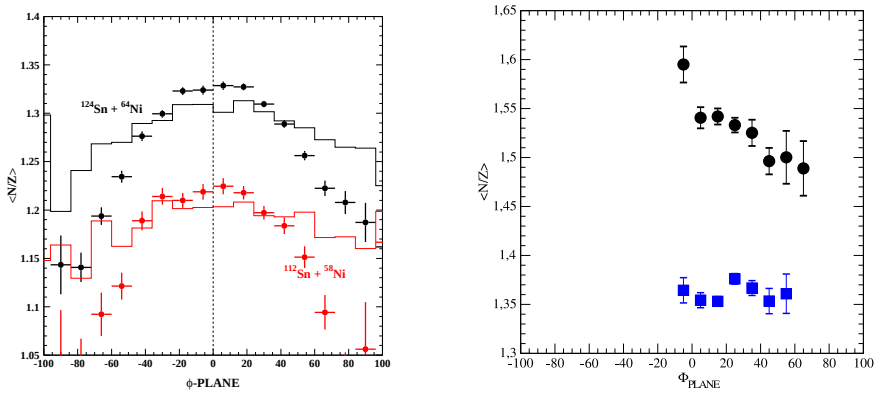

Figure 5: Correlation between N/Z of IMF and *alignement* in ternary events of the $^{124}Sn+^{64}Ni$ reaction at 35 $AMeV$. *Left Panel*. Exp. results: points correspond to fast formed IMFs (Viola-violation selection); histogram for all IMFs at mid-rapidity (including statistical emissions). *Right Panel*. Simulation results: squares, asysoft; circles, asystiff.

pieces, due to the development of volume (spinodal) and surface instabilities. The formation of a bubble-like configuration is observed, where the initial fragments are located [39].

Fragmentation originates from the break-up of a composite source that expands with a given velocity field. Since neutrons and protons experience different forces, one may expect a different radial flow for the two species. In this case, the N/Z composition of the source would not be uniform, but would depend on the radial distance from the center or mass or, equivalently, on the local velocity. This trend should then be reflected in a clear correlation between isospin content and kinetic energy of the formed IMF's, [38].

This observable is plotted in Fig.4 (Right Panel) for the three reactions. The behaviour observed is rather sensitive to the Iso-EoS. For the proton-rich system, the N/Z decreases with the fragment kinetic energy, expecially in the Asystiff case (left), where the symmetry energy is relatively small at low density. In this case, the Coulomb repulsion pushes the protons towards the surface of the system. Hence, more symmetric fragments acquire larger velocity. The decreasing trend is less pronounced in the Asysoft case (right) because Coulomb effects on protons are counterbalanced by the larger attraction of the symmetry potential. In systems with higher initial asymmetry, the decreasing trend is inversed, due to the larger neutron repulsion in neutron-rich systems.

In conclusion, this analysis reveals the existence of significant, EoS-dependent correlations between the N/Z and the kinetic energy of IMF's produced in central collisions.

4 Isospin Dynamics in Neck Fragmentation at Fermi Energies

It is now quite well established that the largest part of the reaction cross section for dissipative collisions at Fermi energies goes through the *Neck Fragmentation* channel, with IMFs directly produced in the interacting zone in semiperipheral collisions on very short time scales [40, 6]. We can predict interesting isospin transport effects for this new fragmentation mechanism since clusters are formed still in a dilute asymmetric matter but always in contact with the regions of the projectile-like and target-like remnants almost at normal densities. As discussed in Sect.2.2 in presence of density gradients the isospin transport is mainly ruled by drift coefficients and so we expect a larger neutron flow to the neck clusters for a stiffer symmetry energy around saturation, [5, 41]. The isospin dynamics can be directly extracted from correlations between N/Z, *alignement* and emission times of the IMFs. The alignment between $PLF-IMF$ and $PLF-TLF$ directions represents a very convincing evidence of the dynamical origin of the mid-rapidity fragments produced on short time scales [42]. The form

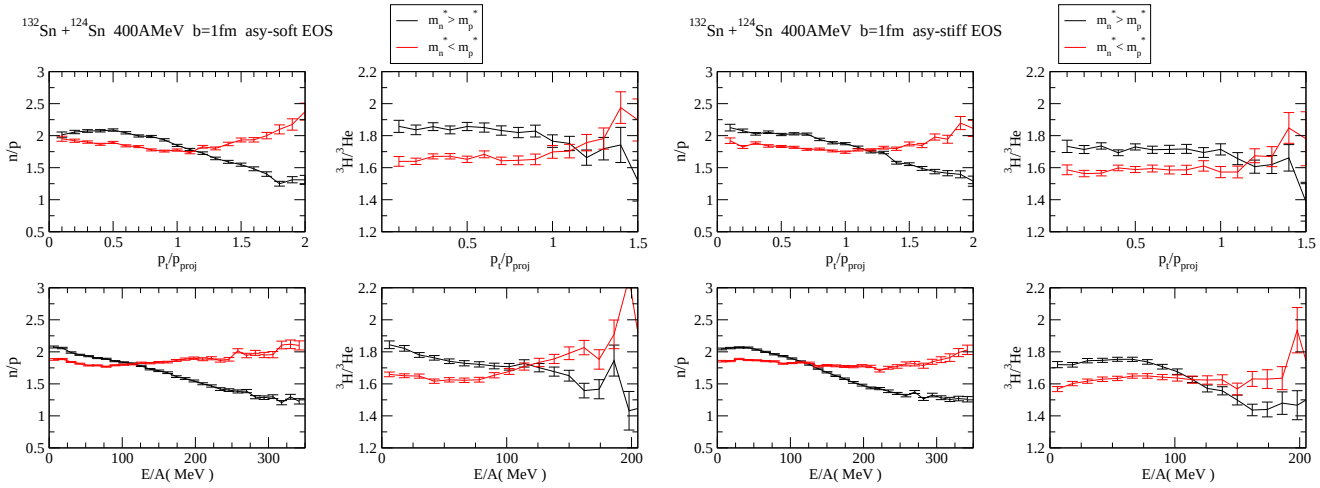

Figure 6: 132Sn+124Sn at 400AMeV, central coll.Isospin content of nucleon and light ion emissions vs p_t (upper) and kinetic energy (lower). Upper Panel: Asysoft; Lower Panel: Asystiff.

of the Φ_{plane} distributions (centroid and width) can give a direct information on the fragmentation mechanism [43]. Recent calculations confirm that the light fragments are emitted first, a general feature expected for that rupture mechanism [45]. The same conclusion can be derived from *direct* emission time measurements based on deviations from Viola systematics observed in event-by-event velocity correlations between IMFs and the PLF/TLF residues [42, 43, 44]. We can figure out a continuous transition from fast produced fragments via neck instabilities to clusters formed in a dynamical fission of the projectile(target) residues up to the evaporated ones (statistical fission). Along this line it would be even possible to disentangle the effects of volume and shape instabilities. A neutron enrichment of the overlap ("neck") region is expected, due to the neutron migration from higher (spectator) to lower (neck) density regions, directly related to the slope of the symmetry energy [45].

A very nice new analysis has been performed on the $Sn + Ni$ data at 35 $AMeV$ by the Chimera Collab.,[46], see Fig.5 left panel. A strong correlation between neutron enrichement and alignement (when the short emission time selection is enforced) is seen, that can be reproduced only with a stiff behavior of the symmetry energy, Fig.3 right panel (for primary fragments) [47]. This represents a clear evidence in favor of a relatively large slope (symmetry pressure) around saturation. We note a recent confirmation from structure data, i.e. from monopole resonances in Sn-isotopes [48].

5 Isospin Effects at High Baryon Density: Effective Mass Splitting and Collective Flows

The problem of Momentum Dependence in the Isovector channel ($Iso - MD$) is still very controversial and it would be extremely important to get more definite experimental information, see the recent refs. [49, 50, 51]. Exotic Beams at intermediate energies are of interest in order to have high momentum particles and to test regions of high baryon (isoscalar) and isospin (isovector) density during the reaction dynamics. Our transport code has been implemented with a $BGBD - like$ [54, 55] mean field with a different (n, p) momentum dependence, see [50, 51]. This will allow to follow the dynamical effect of opposite n/p effective mass splitting while keeping the same density dependence of the symmetry energy [34].

We present here some preliminary results for reactions induced by ^{132}Sn beams on ^{124}Sn targets at $400AMeV$ [52]. For central collisions in the interacting zone we can reach baryon densities about $1.7 - 1.8\rho_0$ in a transient time of the order of 15-20 fm/c. The system is quickly expanding and the

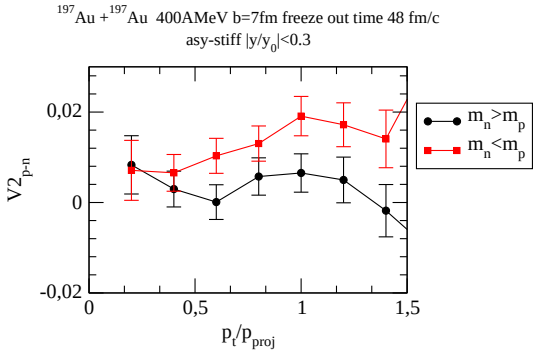

Figure 7: Transverse momentum dependence of the difference between proton and neutron V_2 flows, at mid-rapidity, in a semi-central reaction Au+Au at 400AMeV.

Freeze-Out time is around 50fm/c.

In Fig.6 we present the (n/p) and $^3H/^3He$ yield ratios at freeze-out, for two choices of Asy-stiffness and mass splitting, vs. transverse momentum (upper curves) and kinetic energy (lower curves). In this way we can separate particle emissions from sources at different densities. We note two interesting features: i) the curves are crossing at $p_t \simeq p_{projectile} = 2.13 fm^{-1}$; ii) the effect is not much dependent on the stiffness of the symmetry term. The crossing nicely corresponds to a source at baryon density $\rho \simeq 1.6\rho_0$, [50, 51]. These data seem to be suitable to disentangle $Iso-MD$ effects.

Collective flows are very good candidates since they are expected to be very sensitive to the momentum dependence of the mean field, see [53, 5]. The transverse flow, $V_1(y,p_t) = \langle \frac{p_x}{p_t} \rangle$, provides information on the anisotropy of nucleon emission on the reaction plane. Very important for the reaction dynamics is the elliptic flow, $V_2(y,p_t) = \langle \frac{p_x^2 - p_y^2}{p_t^2} \rangle$. The sign of V_2 indicates the azimuthal anisotropy of emission: on the reaction plane ($V_2 > 0$) or out-of-plane ($squeeze-out$, $V_2 < 0$) [53]. We have then tested the $Iso-MD$ of the fields just evaluating the $Difference$ of neutron/proton transverse and elliptic flows $V_{1,2}^{(n-p)}(y,p_t) \equiv V_{1,2}^n(y,p_t) - V_{1,2}^p(y,p_t)$ at various rapidities and transverse momenta in semicentral $(b/b_{max} = 0.5)$ $^{197}Au + ^{197}Au$ collisons at $400 AMeV$. For the nucleon elliptic flows the mass splitting effect is evident at all rapidities, and nicely increasing at larger rapidities and transverse momenta, with more neutron flow when $m_n^* < m_p^*$. From Fig.7 we clearly see how at mid-rapidity the mass splitting effects are more evident for higher tranverse momentum selections, i.e. for high density sources. In particular the elliptic flow difference becomes negative when $m_n^* < m_p^*$, revealing a faster neutron emission and so more neutron squeeze out (more spectator shadowing). In correspondance the proton flow is more negative (more proton squeeeze out) when $m_n^* > m_p^*$. It is however difficult to draw definite conclusions only from proton data. The measurement of n/p flow differences appears essential. Due to the difficulties in measuring neutrons, our suggestion is to measure the difference between light isobar flows, like ^3H vs. ^3He and so on. We expect to still see effective mass splitting effects.

6 Isospin Effects on Meson Production in Relativistic Heavy Ion Collisions

The phenomenology of isospin effects on heavy ion reactions at intermediate energies (few $AGeV$ range) is extremely rich and can allow a "direct" study of the covariant structure of the isovector interaction in a high density hadron medium. We work within a relativistic transport frame, beyond the cascade picture, consistently derived from effective Lagrangians, where isospin effects are accounted for in the mean field and collision terms. We show that rather sensitive observables are provided by the pion/kaon production (π^-/π^+, K^0/K^+ yields). Relevant non-equilibrium effects are stressed.

An effective Lagrangian approach to the hadron interacting system is extended to the isospin degree

of freedom: within the same frame equilibrium properties (EoS, [56]) and transport dynamics can be consistently derived. Within a covariant picture of the nuclear mean field, for the description of the symmetry energy at saturation (a_4 parameter of the Weizsäecker mass formula) (a) only the Lorentz vector ρ mesonic field, and (b) both, the vector ρ (repulsive) and scalar δ (attractive) effective fields are included. In the latter case a rather intuitive form of the Symmetry Energy can be obtained [12, 13]

$$E_{sym} = \frac{1}{6}\frac{k_F^2}{E_F} + \frac{1}{2}\left[f_\rho - f_\delta\left(\frac{m^*}{E_F}\right)^2\right]\rho_B. \quad . \tag{9}$$

The competition between scalar and vector fields leads to a stiffer symmetry term at high density [12, 5].

We present here observable effects in the dynamics of heavy ion collisions. We focus our attention on the isospin content of meson production. The starting point is a simple phenomenological version of the Non-Linear (with respect to the iso-scalar, Lorentz scalar σ field) effective nucleon-boson field theory, the Quantum-Hadro-Dynamics [56]. According to this picture the presence of the hadronic medium leads to effective masses and momenta $M^* = M + \Sigma_s$, $k^{*\mu} = k^\mu - \Sigma^\mu$, with Σ_s, Σ^μ scalar and vector self-energies. For asymmetric matter the self-energies are different for protons and neutrons, depending on the isovector meson contributions. We will call the corresponding models as $NL\rho$ and $NL\rho\delta$, respectively, and just NL the case without isovector interactions. For the more general $NL\rho\delta$ case the self-energies of protons and neutrons read:

$$\begin{aligned} \Sigma_s(p,n) &= -f_\sigma\sigma(\rho_s) \pm f_\delta\rho_{s3}, \\ \Sigma^\mu(p,n) &= f_\omega j^\mu \mp f_\rho j_3^\mu, \end{aligned} \tag{10}$$

(upper signs for neutrons), where $\rho_s = \rho_{sp} + \rho_{sn}$, $j^\alpha = j_p^\alpha + j_n^\alpha, \rho_{s3} = \rho_{sp} - \rho_{sn}$, $j_3^\alpha = j_p^\alpha - j_n^\alpha$ are the total and isospin scalar densities and currents and $f_{\sigma,\omega,\rho,\delta}$ are the coupling constants of the various mesonic fields. $\sigma(\rho_s)$ is the solution of the non linear equation for the σ field [12, 5]. From the form of the scalar self-energies we note that in n-rich environment the neutron effective masses are definitely below the proton ones.

For the description of heavy ion collisions we solve the covariant transport equation of the Boltzmann type within the Relativistic Landau Vlasov (RLV) method, using phase-space Gaussian test particles [57], and applying a Monte-Carlo procedure for the hard hadron collisions. The collision term includes elastic and inelastic processes involving the production/absorption of the $\Delta(1232MeV)$ and $N^*(1440MeV)$ resonances as well as their decays into pion channels, [15].

Kaon production has been proven to be a reliable observable for the high density EoS in the isoscalar sector [58, 59]. Here we show that the $K^{0,+}$ production (in particular the K^0/K^+ yield ratio) can be also used to probe the isovector part of the EoS, [16, 60].

Using our RMF transport approach we analyze pion and kaon production in central $^{197}Au + ^{197}Au$ collisions in the $0.8 - 1.8$ $AGeV$ beam energy range, comparing models giving the same "soft" EoS for symmetric matter and with different effective field choices for E_{sym}.

Fig. 8 reports the temporal evolution of $\Delta^{\pm,0,++}$ resonances, pions ($\pi^{\pm,0}$) and kaons ($K^{+,0}$) for central Au+Au collisions at $1AGeV$.

It is clear that, while the pion yield freezes out at times of the order of $50fm/c$, i.e. at the final stage of the reaction (and at low densities), kaon production occurs within the very early (compression) stage, and the yield saturates at around $20fm/c$. From Fig. 8 we see that the pion results are weakly dependent on the isospin part of the nuclear mean field. However, a slight increase (decrease) in the π^- (π^+) multiplicity is observed when going from the NL to the $NL\rho$ and then to the $NL\rho\delta$ model, i.e. increasing the vector contribution f_ρ in the isovector channel. This trend is more pronounced for kaons, see the right panel, due to the high density selection of the source and the proximity to the production threshold. Consistently, as shown in the insert, larger effects are expected for early emitted kaons, reflecting the early N/Z of the system.

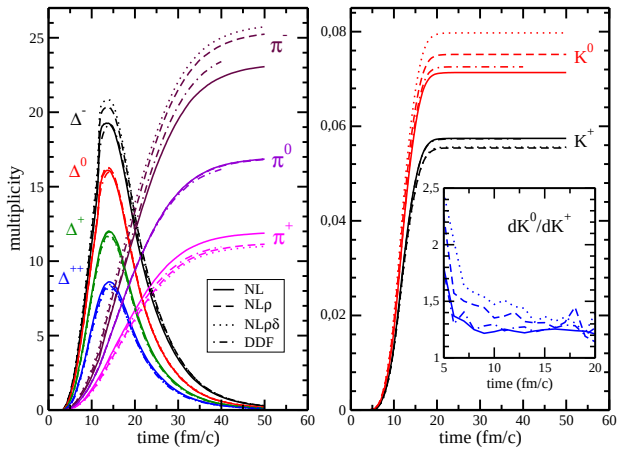

Figure 8: Time evolution of the $\Delta^{\pm,0,++}$ resonances and pions $\pi^{\pm,0}$ (left), and kaons ($K^{+,0}$ (right) for a central ($b = 0$ fm impact parameter) Au+Au collision at 1 AGeV incident energy. Transport calculation using the $NL, NL\rho, NL\rho\delta$ and DDF models for the iso-vector part of the nuclear EoS are shown. The inset contains the differential K^0/K^+ ratio as a function of the kaon emission time.

When isovector fields are included the symmetry potential energy in neutron-rich matter is repulsive for neutrons and attractive for protons. In a HIC this leads to a fast, pre-equilibrium, emission of neutrons. Such a *mean field* mechanism, often referred to as isospin fractionation [5], is responsible for a reduction of the neutron to proton ratio during the high density phase, with direct consequences on particle production in inelastic NN collisions. *Threshold* effects represent a more subtle point. The energy conservation in a hadron collision in general has to be formulated in terms of the canonical momenta, i.e. for a reaction $1 + 2 \rightarrow 3 + 4$ as $s_{in} = (k_1^\mu + k_2^\mu)^2 = (k_3^\mu + k_4^\mu)^2 = s_{out}$. Since hadrons are propagating with effective (kinetic) momenta and masses, an equivalent relation should be formulated starting from the effective in-medium quantities $k^{*\mu} = k^\mu - \Sigma^\mu$ and $m^* = m + \Sigma_s$, where Σ_s and Σ^μ are the scalar and vector self-energies, Eqs.(10). The self-energy contributions will influence the particle production at the level of thresholds as well as of the phase space available in the final channel. In fact the *threshold* effect is dominant and consequently the results are nicely sensitive to the covariant structure of the isovector fields. At each beam energy we see an increase of the π^-/π^+ and K^0/K^+ yield ratios with the models $NL \rightarrow DDF \rightarrow NL\rho \rightarrow NL\rho\delta$. The effect is larger for the K^0/K^+ compared to the π^-/π^+ ratio. This is due to the subthreshold production and to the fact that the isospin effect enters twice in the two-step production of kaons, see [16]. Interestingly the Iso-EoS effect for pions is increasing at lower energies, when approaching the production threshold.

We have to note that in a previous study of kaon production in excited nuclear matter the dependence of the K^0/K^+ yield ratio on the effective isovector interaction appears much larger (see Fig.8 of ref.[15]). The point is that in the non-equilibrium case of a heavy ion collision the asymmetry of the source where kaons are produced is in fact reduced by the $n \rightarrow p$ "transformation", due to the favored $nn \rightarrow p\Delta^-$ processes. This effect is almost absent at equilibrium due to the inverse transitions, see Fig.3 of ref.[15]. Moreover in infinite nuclear matter even the fast neutron emission is not present. This result clearly shows that chemical equilibrium models can lead to uncorrect results when used for transient states of an *open* system.

7 On the Transition to a Mixed Hadron-Quark Phase at High Baryon and Isospin Density

The possibility of the transition to a mixed hadron-quark phase, at high baryon and isospin density, is finally suggested. Some signatures could come from an expected "neutron trapping" effect.

In order to check the possibility of observing some precursor signals of a new physics even in collisions

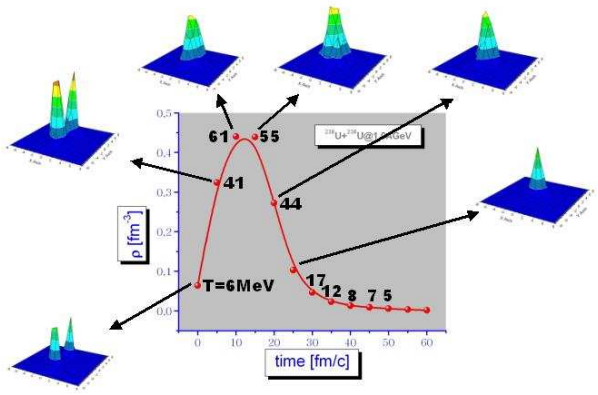

Figure 9: $^{238}U +^{238} U$, 1 $AGeV$, semicentral. Correlation between density, temperature (black values), momentum thermalization (3-D plots), inside a cubic cell, 2.5 fm wide, in the center of mass of the system.

of stable nuclei at intermediate energies we have performed some event simulations for the collision of very heavy, neutron-rich, elements. We have chosen the reaction $^{238}U +^{238} U$ (average proton fraction $Z/A = 0.39$) at 1 $AGeV$ and semicentral impact parameter $b = 7$ fm just to increase the neutron excess in the interacting region. In Fig. 9 we report the evolution of momentum distribution and baryon density in a space cell located in the c.m. of the system. We see that after about 10 fm/c a local equilibration is achieved. We have a unique Fermi distribution and from a simple fit we can evaluate the local temperature (black numbers in MeV). We note that a rather exotic nuclear matter is formed in a transient time of the order of 10 fm/c, with baryon density around $3 - 4\rho_0$, temperature $50 - 60$ MeV, energy density 500 MeV fm^{-3} and proton fraction between 0.35 and 0.40, likely inside the estimated mixed phase region.

In fact we can study the isospin dependence of the transition densities [17]. The structure of the mixed phase is obtained by imposing the Gibbs conditions [62] for chemical potentials and pressure and by requiring the conservation of the total baryon and isospin densities

$$\begin{aligned}
&\mu_B^{(H)} = \mu_B^{(Q)}\,, \quad \mu_3^{(H)} = \mu_3^{(Q)}\,,\\
&P^{(H)}(T, \mu_{B,3}^{(H)}) = P^{(Q)}(T, \mu_{B,3}^{(Q)})\,,\\
&\rho_B = (1-\chi)\rho_B^H + \chi\rho_B^Q\,,\\
&\rho_3 = (1-\chi)\rho_3^H + \chi\rho_3^Q\,,
\end{aligned} \tag{11}$$

where χ is the fraction of quark matter in the mixed phase.

In this way we get the *binodal* surface which gives the phase coexistence region in the (T, ρ_B, ρ_3) space. For a fixed value of the conserved charge ρ_3 we will study the boundaries of the mixed phase region in the (T, ρ_B) plane. In the hadronic phase the charge chemical potential is given by $\mu_3 = 2E_{sym}(\rho_B)\frac{\rho_3}{\rho_B}$. Thus, we expect critical densities rather sensitive to the isovector channel in the hadronic EoS.

In Fig. 10 we show the crossing density ρ_{cr} separating nuclear matter from the quark-nucleon mixed phase, as a function of the proton fraction Z/A. We can see the effect of the δ-coupling towards an *earlier* crossing due to the larger symmetry repulsion at high baryon densities. In the same figure we report the paths in the $(\rho, Z/A)$ plane followed in the c.m. region during the collision of the n-rich ^{132}Sn+^{132}Sn system, at different energies. At 300 $AMeV$ we are just reaching the border of the mixed phase, and we are well inside it at 1 $AGeV$.

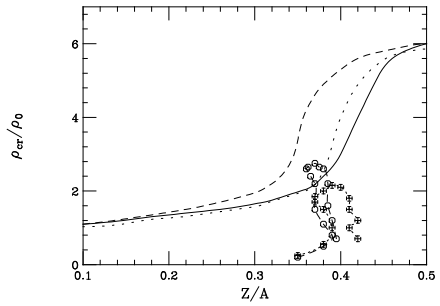

Figure 10: Variation of the transition density with proton fraction for various hadronic EoS parameterizations. Dotted line: $GM3$ RMF-model [61]; dashed line: $NL\rho$; solid line: $NL\rho\delta$. For the quark EoS: MIT bag model with $B^{1/4}$=150 MeV. The points represent the path followed in the interaction zone during a semi-central ^{132}Sn+^{132}Sn collision at 1 $AGeV$ (circles) and at 300 $AMeV$ (crosses).

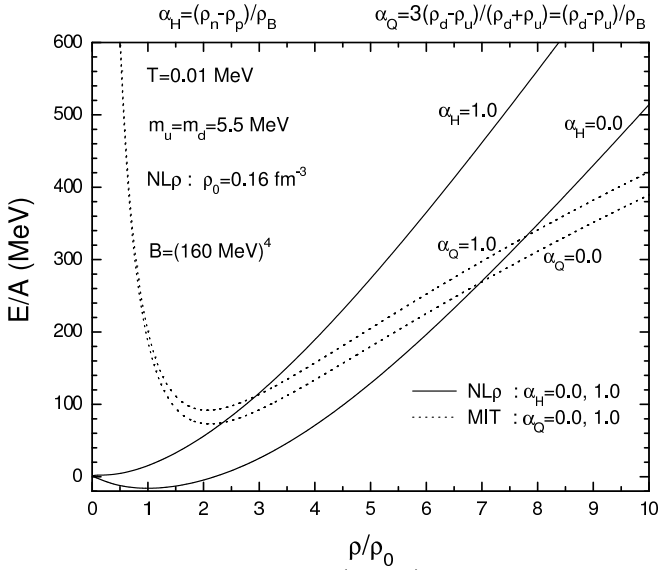

Figure 11: EoS of Simmetric/Neutron Matter: Hadron ($NL\rho$), solid lines, vs. Quark (MIT-Bag), dashed lines. $\alpha_{H,Q}$ represent the isospin asymmetry parameters respectively of the hadron,quark matter: $\alpha_{H,Q}=0$, Symmetric Matter; $\alpha_{H,Q}=1$, Neutron Matter.

We can expect a *neutron trapping* effect, supported by statistical fluctuations as well as by a symmetry energy difference in the two phases. In fact while in the hadron phase we have a large neutron potential repulsion (in particular in the $NL\rho\delta$ case), in the quark phase we only have the much smaller kinetic contribution. Observables related to such neutron "trapping" could be an inversion in the trend of the formation of neutron rich fragments and/or of the π^-/π^+, K^0/K^+ yield ratios for reaction products coming from high density regions, i.e. with large transverse momenta.

Isospin in Effective Partonic Models

From the above discussion it appears extremely important to include the Isospin degree of freedom in any effective approach to the QCD dynamics. This can be easily performed in a two-flavor NJL model [63] where the isospin asymmetry can be included in a flavor-mixing picture [64] via a Gap Equation like $M_i = m_i - 4G_1\Phi_i - 4G_2\Phi_j$, $i \neq j, (u,d)$, where the $\Phi_{u,d} =< \bar{u}u >, < \bar{d}d >$ are the two (negative) condensates and $m_{u,d} = m$ the (equal) current masses. Introducing explicitily a flavor mixing, i.e. the dependence of the constituent mass of a given flavor to both condensate, via $G_1 = (1-\alpha)G_0, G_2 = \alpha G_0$ we have the coupled equations

$$M_u = m - 4G_0\Phi_u - 4\alpha G_0(\Phi_u - \Phi_d),$$

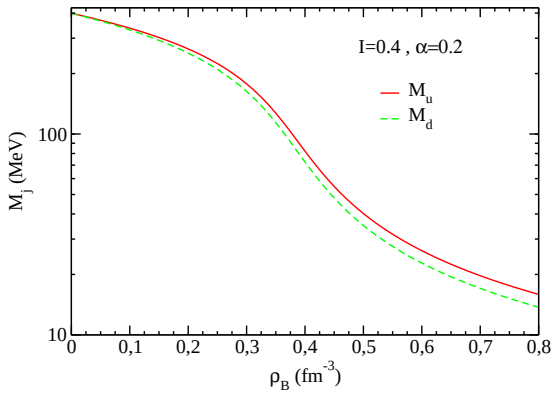

Figure 12: NJL results with flavor mixing $\alpha = 0.2$ and isospin asymmetry $(N-Z)/A = 0.4$: costituent u- d- masses vs.baryon density.

$$M_d = m - 4G_0\Phi_u + 4(1-\alpha)G_0(\Phi_u - \Phi_d). \tag{12}$$

For $\alpha = 1/2$ we have back the usual NJL ($M_u = M_d$), while small/large mixing is for $\alpha \Rightarrow 0/\alpha \Rightarrow 1$ respectively.

In neutron rich matter $\mid \Phi_d \mid$ decreases more rapidly due to the larger ρ_d and so $(\Phi_u - \Phi_d) < 0$. In the "realistic" small mixing case, see also [64, 65], we will get a definite $M_u > M_d$ splitting at high baryon density (before the chiral restoration). This expectation is nicely confirmed by a full calculation [66] of the coupled gap equations with standard parameters (same as in ref.[64]). The results are shown in Fig.12.

All that represents a more fundamental confirmation of the $m_p^* > m_n^*$ choice in the hadron phase, as suggested by the effective QHD model with the isovector scalar δ coupling, see before and [12]. However this can represent just a very first step towards a more complete treatment of isovector interactions in effective partonic models, of large interest for the discussion of the phase transition at high densities. We can easily see that the mass splitting effect is not changing much the symmetry energy in the quark phase addressed before. However confinement is still missing in these mean field models. Stimulating new perspectives are open.

8 Perspectives

We have shown that *violent* collisions of n-rich heavy ions from low to relativistic energies can bring new information on the isovector part of the in-medium interaction, qualitatively different from equilibrium EoS properties. We have presented quantitative results in a wide range of beam energies. At low energies we see isospin effects on the dissipation in fusion and deep inelastic collisions, at Fermi and Intermediate energies the Iso-EoS sensitivity of the isospin dynamics in fragment reactions and in collective flows.

We have shown that meson production in n-rich heavy ions collisions at intermediate energies can bring new information on the isovector part of the in-medium interaction at high baryon densities. Important non-equilibrium effects for particle production are stressed. Finally the possibility of observing precursor signals of the phase transition to a mixed hadron-quark matter at high baryon density is suggested.

10 years after the first studies of Iso-EoS effects on reactions [3] the symmetry energy case is still open. The results presented in this "Isospin Journey" appear very promising for the possibility of exciting new data from dissipative collisions with radioactive beams.

Aknowledgements

We warmly thank A.Drago and A.Lavagno for the collaboration on the mixed hadron-quark phase transition at high baryon and isospin density.

One of authors, V. B. thanks for warm hospitality at Laboratori Nazionali del Sud, INFN. This work was supported in part by the Romanian Ministery for Education and Research under the contracts PNII, No. ID-946/2007.

References

[1] C.Fuchs, H.H.Wolter, *Eur. Phys. Jour.* **A30** (2006) 5.

[2] S.Fantoni et al., AIP Conf.Proc. **1056** (2008) 233-240 and arXiv:0807.543[nucl-th].

[3] M. Colonna, M. Di Toro, G. Fabbri, S. Maccarone, Phys. Rev. **C57** (1998) 1410

[4] *Isospin Physics in Heavy-ion Collisions at Intermediate Energies*, Eds. B.A. Li and W. Udo Schröder, Nova Science Publishers (2001, New York)

[5] V.Baran, M.Colonna, V.Greco, M.Di Toro, *Phys. Rep.* **410** (2005) 335.

[6] M.Di Toro, A.Olmi, R.Roy, *Eur. Phys. Jour.* **A30** (2006) 65.

[7] M.Colonna and M.B.Tsang, Eur. Phys. J. **A30** (2006) 165, and refs. therein.

[8] B.A. Li, L.W. Chen, C.M. Ko, *Phys. Rep.* **465** (2008) 113.

[9] A.Guarnera, M.Colonna, P.Chomaz, *Phys. Lett.* **B373** (1996) 267.

[10] M.Colonna et al., *Nucl. Phys.* **A642** (1998) 449.

[11] P.Chomaz, M.Colonna, J.Randrup, *Phys. Rep.* **389** (2004) 263.

[12] B.Liu et al., *Phys. Rev.* **C65** (2002) 045201.

[13] T.Gaitanos et al., *Nucl. Phys.* **A732** (2004) 24.

[14] E.Santini, T.Gaitanos, M.Colonna, M.Di Toro, *Nucl. Phys.* **A756** (2005) 468.

[15] G.Ferini, M.Colonna, T.Gaitanos, M.Di Toro, *Nucl. Phys.* **A762** (2005) 147.

[16] G.Ferini, T.Gaitanos, M.Colonna, M.Di Toro, H.H.Wolter, *Phys. Rev. Lett.* **97** (2006) 202301.

[17] M.Di Toro, A.Drago, T.Gaitanos, V.Greco, A.Lavagno, *Nucl. Phys.* **A775** (2006) 102.

[18] V. Baran et al., *Nucl. Phys.* **A703** (2002) 603.

[19] P. Chomaz, M. Di Toro, A.Smerzi, *Nucl. Phys.* **A563** (1993) 509.

[20] P. F. Bortignon et al., *Nucl. Phys.* **A583** (1995) 101c.

[21] D. Pierroutsakou et al., *Phys. Rev.* **C71** (2005) 054605.

[22] B.Martin, D. Pierroutsakou et al. (Medea Collab.), *Phys. Lett.* **664** (2008) 47.

[23] D. M. Brink and M. Di Toro,, *Nucl. Phys.* **A372** (1981) 151.

[24] V. Baran, D. M. Brink, M. Colonna, M. Di Toro, *Phys. Rev. Lett.* **87** (2001) 182501

[25] M.Di Toro et al., *Int.Jou.Mod.Phys.* **E17** (2008) 110.

[26] M.Lewitovicz, *Nucl.Phys.* **A805** (2008) 519c.

[27] Letter of Intent for the new SPIRAL2 Facility at GANIL.

[28] V.Baran, C.Rizzo, M.Colonna, M.Di Toro, D.Pierroutsakou, *The Dynamical Dipole Mode in Fusion Reactions with Exotic Nuclear Beams*, arXiv:0807.4118[nucl-th].

[29] M.Zielinska-Pfabe et al, *Isospin Properties of fast Light Particles*, IWM Int.Workshop, SIF, Conf.Proc.Vol. 95 (2008) p. 303-310.

[30] V.Baran et al., *Phys.Rev.* **C72** (2005) 064620.

[31] F.Rami et al., *Phys.Rev.Lett.* **84** (2000) 1120.

[32] M.B. Tsang, et al., Phys. Rev. Lett. **92**, 062701 (2004)

[33] B.A. Li, L.W. Chen, Phys. Rev. C **72**, 064611 (2005);
L.W. Chen, C.M. Ko, B.A. Li, Phys. Rev. Lett **94**, 032701 (2005)

[34] J.Rizzo et al., *Nucl.Phys.* **A806** (2008)79-104.

[35] H.Mueller and B.D.Serot, *Phys.Rev.* **C52** (1995) 2072.

[36] Bao-An Li and C.M.Ko, *Nucl.Phys.* **A618** (1997) 498.

[37] V. Baran et al., *Nucl.Phys.* **A632** (1998) 287.

[38] M.Colonna et al., *Isospin Distillation with Radial Flow* arXiv:0707.3092 [nucl-th].

[39] M.Colonna et al., *Nucl.Phys.* **A742** (2004) 337.

[40] M.Colonna, M.Di Toro, A.Guarnera, *Nucl. Phys.* **A589** (1995) 160.

[41] V.Baran et al.,, *Phys. Rev.* **C72** (2005) 064620.

[42] V.Baran, M.Colonna, M.Di Toro, *Nucl. Phys.* **A730** (2004) 329.

[43] E.De Filippo et al. (Chimera Collab.), *Phys. Rev.* **C71** (2005) 044602; *Phys. Rev.* **C71** (2005) 064604.

[44] J.Wilczynski et al. (Chimera Collab.), *Int. Jour. Mod. Phys.* **E14** (2005) 353.

[45] R.Lionti, V.Baran, M.Colonna, M.Di Toro, *Phys. Lett.* **B625** (2005) 33.

[46] E. De Filippo et al. (Chimera Collab.), *Time scales and isospin effects on reaction dynamics*, NN06 Conf., Rio de Janeiro, August 2006, and *Isospin signals in reaction dynamics*, Int.Conf.on Nuclear Fragmentation, Antalya 2007.

[47] V.Baran, M.Colonna, M.Di Toro, *Hierarchy in Mid-Rapidity Fragmentation: Mass, Charge, Velocity Correlations*, 2008 in preparation.

[48] T.Li, U.Garg et al., *Phys. Rev. Lett.* **99** (2007) 162503.

[49] B.-A. Li, B.Das Champak, S.Das Gupta, C.Gale, *Nucl. Phys.* **A735** (2004) 563.

[50] M.Di Toro, M.Colonna, J.Rizzo, AIP Conf.Proc.**791** (2005) 70-83

[51] J.Rizzo, M.Colonna, M.Di Toro *Phys. Rev.* **C72** (2005) 064609.

[52] Valentina Giordano, Master Thesis, Univ. of Catania 2008.

[53] P. Danielewicz, *Nucl. Phys.* **A673** (2000) 375.

[54] C.Gale, G.F.Bertsch, S.Das Gupta, *Phys.Rev.* **C41** (1990) 1545.

[55] I.Bombaci et al., *Nucl.Phys.* **A583** (1995) 623.

[56] B. D. Serot, J. D. Walecka, Advances in Nuclear Physics, **16**, 1, eds. J. W. Negele, E. Vogt, (Plenum, N.Y., 1986).

[57] C. Fuchs. H.H. Wolter, *Nucl. Phys.* **A589** (1995) 732.

[58] C. Fuchs, *Prog.Part.Nucl.Phys.* **56** 1-103 (2006).

[59] C.Hartnack, H.Oeschler, J.Aichelin, *Phys. Rev. Lett.* **96** (2006) 012302.

[60] V.Prassa et al., *Nucl.Phys.* **A789** (2007) 311.

[61] N.K.Glendenning, S.A.Moszkowski, *Phys. Rev. Lett.* **67** (1991) 2414.

[62] L.D.Landau, L.Lifshitz, *Statistical Physics*, Pergamon Press, Oxford 1969.

[63] Y.Nambu, G.Jona-Lasinio, *Phys. Rev.* **122** (1061) 345; **124** (1061) 246.

[64] M.Frank, M.Buballa, M.Oertel, *Phys. Lett.* **B562** (2003) 221.

[65] Guo-yun Shao et al., *Phys. Rev.* **D73** (2006) 076003.

[66] S.Plumari, Ph.D.Thesis, Univ.Catania 2008.

arXiv:0811.2880v1 [nucl-th] 18 Nov 2008

New Nuclei around the N = Z in the A = 80-90 region

N. Marginean,[1,2] C. Rossi Alvarez,[3] D. Bucurescu,[2] C. A. Ur,[3,2]
A. Gadea,[4] S. Lunardi,[3] D. Bazzacco,[3] G. de Angelis,[1] M. Axiotis,[1]
M. De Poli,[1] E. Farnea,[1,3] M. Ionescu-Bujor,[2] A. Iordachescu,[2] S. M. Lenzi,[3]
Th. Kröll,[1,3] T. Martinez,[1] R. Menegazzo,[3] D. R. Napoli,[1]
G. Nardelli,[5] P. Pavan,[3] B. Quintana,[3,6] P. Spolaore[1]

[1]INFN, Laboratori Nazionali di Legnaro, Italy
[2]H. Hulubei National Inst. for Phys. and Nucl. Eng., Bucharest, Romania
[3]Dipartimento di Fisica dell'Università and INFN, Sez. di Padova, Italy
[4]Instituto de Fisica Corpuscular, Valencia, Spain
[5]Dip. di Chi. Fis. dell'Università di Venezia and INFN, Sez. di Padova, Italy
[6] Grupo de Fisica Nuclear, Universidad de Salamanca, Spain

November 18, 2008

Abstract

Correlations in the nuclear wave-function beyond the mean-field or Hartree-Fock approximation are very important to describe basic properties of nuclear structure. Various approaches to account for such correlations are described and compared to each other. This includes the hole-line expansion, the coupled cluster or "exponential S" approach, the self-consistent evaluation of Greens functions, variational approaches using correlated basis functions and recent developments employing quantum Monte-Carlo techniques. Details of these correlations are explored and their sensitivity to the underlying nucleon-nucleon interaction. Special attention is paid to the attempts to investigate these correlations in exclusive nucleon knock-out experiments induced by electron scattering. Another important issue of nuclear structure physics is the role of relativistic effects as contained in phenomenological mean field models. The sensitivity of various nuclear structure observables on these relativistic features are investigated. The report includes the discussion of nuclear matter as well as finite nuclei.

1 Introduction

One of the central challenges of theoretical nuclear physics is the attempt to describe the basic properties of nuclear systems in terms of a realistic nucleon-nucleon (NN) interaction. Such an attempt typically contains two major steps. In the first step one has to consider a specific model for the NN interaction. This could be a model which is inspired by the quantum-chromo-dynamics[**?**], a meson-exchange or One-Boson-Exchange model[**?**, **?**] or a purely phenomenological ansatz in terms of two-body spin-isospin operators multiplied by local potential functions[**?**, **?**]. Such models are considered as a